11th Australasian Fluid Mechanics Conference
University of Tasmania, Hobart, Australia
14-18 December 1992

RESPONSE OF A MOVABLE WALL TO A SHOCK WAVE

S.M. NABULSI and N.W. PAGE

Department of Mechanical Engineering
University of Queensland
QLD 4072, AUSTRALIA

ABSTRACT

This paper describes a study of the response of a movable wall to an incident shock. The subsequent motion of the movable wall is considered in terms of the choice of gas and initial conditions on either side. Higher initial pressures are shown to be advantageous in developing higher wall accelerations. Gas choice seems to have little effect. Consideration is also given to interaction between the flows generated during the opening of the shock tube diaphragm and a nearby moving wall. The need is established for a probe to monitor local shock strength. A thermocouple probe has been developed to do this. Preliminary results are encouraging.

INTRODUCTION

When a shock wave reflects from an unsupported wall, the pressure differential across the wall causes it to accelerate. As it does so, rarefaction waves are propagated backwards weakening the reflected shock, and compression waves are propagated forwards. These will ultimately coalesce forming a new shock wave in front of the wall. The principal features of this flow are shown in Fig. 1.

Recently there has been growing interest in the flow generated by this shock wave/ wall interaction in widely separated areas of science. One involves the use of a light-weight wall separating the accelerator gas from the test gas in double diaphragm driven free piston expansion tubes (Stalker and Morgan, 1991). Another involves the use of a shock accelerated diaphragm as the macrocarrier in the particle bombardment (biolistic) technique to introduce new genetic material into living cells. A recent review of this technique has been given by Klein et al (1992).

The interaction of a shock wave reflecting at normal incidence to a moving wall was first studied by Meyer (1957) for the case of low strength shocks with negligible entropy rise and with the same gas at the same initial pressures on both sides of the wall. He found good agreement between theory and experiment at least up to incident shocks of shock Mach number 1.5. Morgan and Stalker (1991) developed a simple model which allowed for different gases on either side, but had the simplification that the expansion waves on the upstream side of the wall instantaneously reached the reflected shock so that the region between the reflected shock and moving wall was at the uniform velocity dictated by the wall boundary condition.

This paper describes a study in which the more general treatment of Meyer is extended to allow for different gases across the wall. Consideration is also given to the case where the shock tube diaphragm is in close proximity to the moving wall. This is commonly the geometry adopted for the shock-tube driven technique for genetic engineering mentioned above, the purpose of this close proximity being to exploit rapid reflections of the reflected shock between the contact surface and the upstream surface of the wall so as to maximize acceleration of the wall. Multiple shock reflections between a contact surface and a fixed wall have been studied previously by Bull and Edwards (1968), but no previous study has considered multiple reflection from a moving wall.

An experimental program is outlined to validate approximations made in the modeling of these complex events.

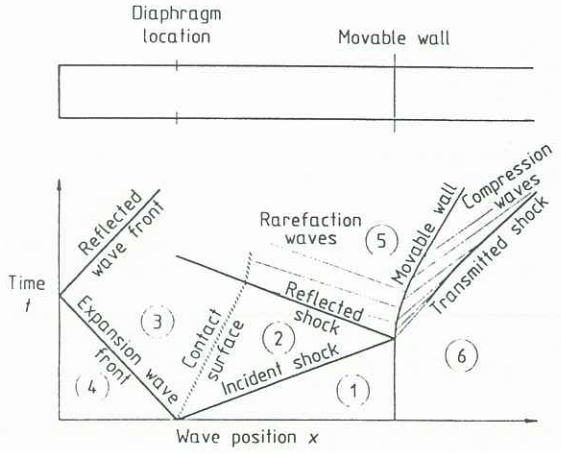

Figure 1. Wave diagram following the impact of a shock wave on a movable wall.

THEORY

(a) Long driven tube

Following Meyer (1957), in the absence of changes to specific entropy, the characteristic equations describing the flow on either side of a wall caused by shock reflection can be written in terms of the Riemann invariants -

$$P = \frac{2}{\gamma - 1} a + u \text{ , constant along } \frac{dx}{dt} = u + a$$

and

$$Q = \frac{2}{\gamma - 1} a - u \text{ , constant along } \frac{dx}{dt} = u - a$$

Here, a and u are the sound and particle speeds and γ is the ratio of specific heats. Since conditions upstream and downstream of the wall are assumed isentropic, Q is constant (Q_6) through the transmitted compression waves and transmitted shock wave, and P is constant (P_2) through the reflected shock and rarefaction waves emanating from the upstream surface of the wall. Thus, the forward (P) characteristics are straight lines downstream of the wall and the backward (Q) characteristics are straight lines upstream of the wall.

At some instant of time, the conditions downstream of the wall will be described by,

$$Q_d = \frac{2}{\gamma - 1} a_d - u_d = Q_6$$

where subscript d refers to conditions at some point on the downstream surface of the wall. Substituting Q_6 into the isentropic relations yields

$$P_d/P_6 = \{ (Q_6 + u_d)/Q_6 \}^{2\gamma_6/(\gamma_6-1)} \quad (1)$$

Similarly at some point c on the upstream surface,

$$P_c/P_{c0} = \{ (P_2 - u_c)/P_2 \}^{2\gamma_2(\gamma_2-1)} \quad (2)$$

where o denotes the condition at t=0. Therefore the pressure difference across the wall is,

$$P_c - P_d = P_{c0}\{(P_2-u_c)/P_2\}^{\alpha 1} - P_6\{(Q_6+u_d)/Q_d\}^{\alpha 2} \quad (3)$$

where $\alpha 1 = 2\gamma_2/(\gamma_2-1)$ and $\alpha 2 = 2\gamma_6/(\gamma_6-1)$. Thus the wall acceleration is given by,

$$du_w/dt = \{(P_c-P_d)/(P_{c0}-P_6)\}\,(du_w/dt)_{t=0}$$

$$= \left(\frac{du_w}{dt}\right)_{t=0} \frac{P_6}{P_{c0}-P_6}\left(\frac{P_{c0}}{P_6}\left(\frac{P_2-u_w}{P_2}\right)^{\alpha 1} - \left(\frac{Q_6+u_w}{Q_6}\right)^{\alpha 2}\right) \quad (4)$$

The above equation can be made non-dimensional by introducing the non-dimensional variables $U=u/a_6$, $A=a/a_6$, $\varepsilon = x/a_6 t_c$, $\tau = t/t_c$, where $t_c = 2a_6/(\gamma_6+1)b$, b is the initial acceleration of the wall. With these and noting that $P_{c0} = P_{50}$, equation 4 becomes,

$$\frac{dU_w}{d\tau} = \frac{2}{\gamma_6+1}\frac{P_6}{P_{50}-P_6}\left(\frac{P_{50}}{P_6}\left(\frac{P'_2-U_w}{P'_2}\right)^{\alpha 1} - \left(\frac{Q'_6+U_w}{Q'_6}\right)^{\alpha 2}\right) \quad (5)$$

where P_{50} and $P'_2 = P_2/a_6$ are determined from the shock equations and now $Q'_6 = 2/(\gamma_6-1)$.

The transmitted shock is determined as follows. The equation of the positive characteristic d-j from some point d on the downstream side of the wall to some point j on the transmitted shock is,

$$\varepsilon_j - \varepsilon_d = (\tau_j - \tau_d)\,(U_d + A_d),$$

Also, $d\varepsilon_j/d\tau_j = M_{sj}$ where M_{sj} is the shock Mach number at j. As U is constant along d-j, normal shock relations lead to,

$$M_{sj} = U_d(\gamma_6+1)/4 + [\{U_d(\gamma_6+1)/4\}^2 + 1]^{1/2} = F(U_d) \quad (6)$$

The boundary conditions are $d\varepsilon_j/d\tau_j = \varepsilon_j = 1$ at $\tau_j = 1$, the point at which the transmitted shock starts which defines the cusp at the beginning of the envelope of the positive characteristics as shown by Courant & Freidrichs (1948).

Similarly, for the reflected shock,

$$\varepsilon_v - \varepsilon_c = (\tau_v - \tau_c)\,(U_c - A_c),$$

$$d\varepsilon_v/d\tau_v = U_2 - A_2 M_v = U_2 - A_2 F\{(U_2-U_c)/A_2)\} \quad (7)$$

The boundary conditions are, $d\varepsilon_v/d\tau_v = U_2 - A_2(M_v)_{\tau=0}$, $\varepsilon_v = 0$ at $\tau_v = 0$. Equations 5, 6 and 7 can be numerically integrated to give the path of the wall, the transmitted shock and the reflected shock in terms of the non-dimensional variables τ and ε. Fig.2 illustrates the results of such calculations, for the special case where the gas upstream of the wall was air and that downstream was helium. The incident shock wave Mach number was 3.6 and the initial pressure of both gases was 5kPa absolute. Both were also initially at room temperature. The effect of the rarefaction waves propagating behind the accelerating wall can clearly be seen. These weaken the reflected shock so that it is ultimately swept forward again. This result was not shown by Meyer who analysed a lower energy wall acceleration.

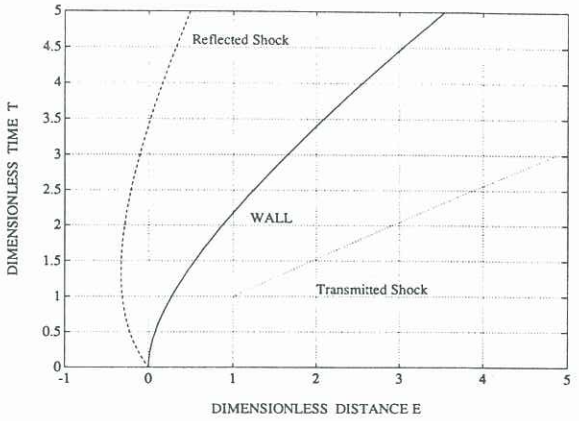

Figure 2. Wave diagram in dimensionless form folllowing the impact of a shock wave (M=3.6) on a 50 micron thick Mylar movable wall.

The motion of the wall would depend on the incident shock strength, the gases on either side and on their initial conditions. To gain more insight into the separate effect of these parameters, we can theoretically explore the behavior of the wall under different conditions using the model described above.

The effect of gas was illustrated by comparing the wall response using either helium or air as the gas downstream. All other conditions were kept the same. The results are shown in Fig.3 as a wave diagram plotted in physical units. For this and subsequent simulations for which the results are given in physical units, the value of initial acceleration (b) used was 6×10^6 ms^{-2}. This corresponds to a 50μm thick Mylar wall. The result indicates that the use of a gas lighter than air (helium) is advantageous over large wall travel distances, however in our present study the travel distance of interest is only about 20mm and it can be seen that no telling advantage can be gained over such a short distance, at least in terms of unrestricted wall acceleration. In applications such as the microprojectile accelerator discussed above, there would be a barrier (stopper plate) preventing the indefinite movement of the wall.

This would also act as a flow restriction so that the simple unrestricted downstream boundary conditions assumed here would not be valid. A more complex analysis of this case may reach different conclusions about the effect of downstream gas.

The effect of varying the initial pressure on both sides of the wall with all other conditions kept the same can be seen in Fig. 4. It is clear from the graph that increasing the pressures P_1 and P_6 results in a pronounced improvement in performance. In fact the initial wall accelerating pressure $P_{50} - P_6$ is doubled when these pressures are doubled.

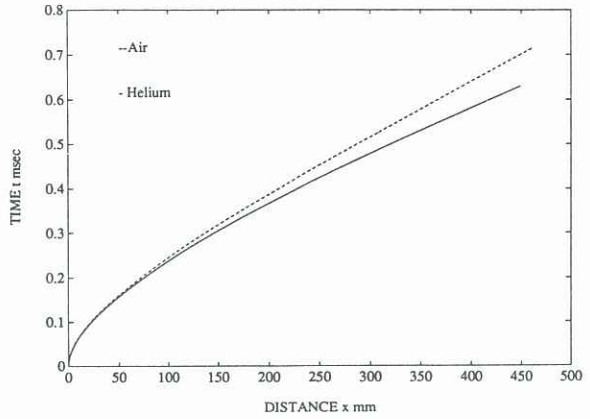

Figure 3. The wall path with helium on the downstream side compared to that with air, with all other conditions kept the same.

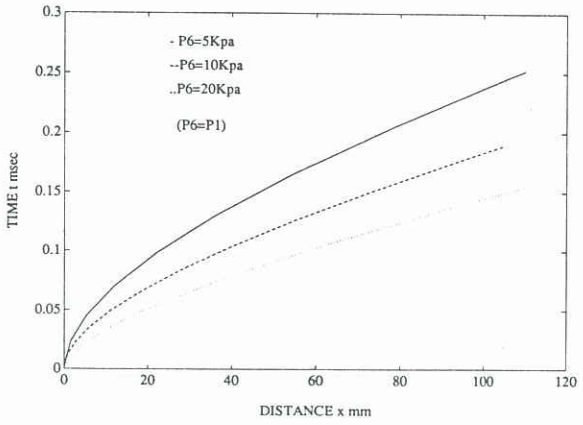

Figure 4. The wall path under different initial pressures on either side of it, with all other conditions kept the same.

(b) Short driven tube

In the application in which the moving wall is a microprojectile accelerator, it has been observed that, by reducing the length of the driven section to less than half a tube diameter, the depth of microprojectile penetration into plant cells is dramatically increased. Due to the close proximity of the bursting diaphram to the movable wall in this configuration, the diaphram opening time will have a significant effect on the performance of the shock tube.

Both Curzon and Phillips (1971) and Simpson et al (1967) devised analytical solutions for the diaphram opening time (t_{op}). These solutions can be used to estimate the diaphragm opening time in the present series of experiments.

The previously published solutions for the diaphragm opening time were based on the following assumptions: (a). The diaphram splits along two diagonals. (b). The petals formed fold back under the action of the high pressure driver gas. (c). The work done in splitting and bending is neglected in comparison to that done by the torque which causes the angular displacement of the petals (i.e petals assumed to behave as freely hinged plates). (d). The pressure acting on a petal is a function of the rotation angle θ i.e $P = P_4 f(\theta)$.

With these assumptions the equation of motion of each petal is -

$$T = I \, d^2\theta/dt^2 \qquad (8)$$

where T is the torque and I, the moment of inertia about the base.

It has been observed in the present work that the aluminum diaphragms used tear into three approximately equal sectors upon rupture. Round diaphragms of 102 mm in diameter are used. For each petal then, $I = 0.467 \, \rho d h^4$ where ρ is the diaphragm material density, d its thickness, and h, the arc width. Assuming $f(\theta)=\cos^2\theta$, equation (8) can be integrated to get,

$$t_{op} = K \, (\rho dh/3.1 \, P_4)^{1/2} \qquad (9)$$

In this analysis we used $f(\theta)=\cos^2\theta$ as used by Simpson et al. (1967) due to the fact that, like us, they used aluminum diaphrams in a round tube which yields K=2.58. In fact, Curzon and Phillips (1971) found that this parameter did not vary much over a wide range of shock diaphragm conditions. With this value,

$$t/t_{op} = 0.548 \int_0^{\theta} (0.5 \sin 2\theta + \theta)^{-1/2} d\theta \qquad (10)$$

where t is the time taken for the petal to rotate through angle θ.

Figure 5 shows the variation of open to total area ratio versus the time to total opening time ratio which is used to determine the area ratio at different times of the opening process.

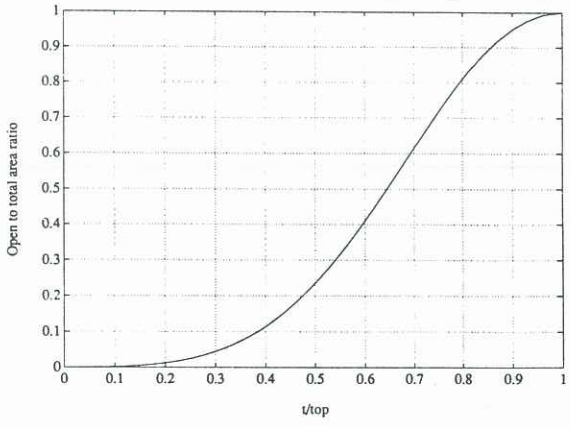

Figure 5. The variation of open to total area ratio versus the time to total opening time ratio for an aluminum daiphram 0.15mm thick.

With the shock tube diaphragm in close proximity to the initial position of the moving wall, the wall will move a significant distance before the diaphragm is fully open. For this phase of the study then, a model is needed of the interaction between an incompletely open shock tube diaphragm and a movable wall. As a starting point in this work, the flow from the incompletely open diaphragm will be modeled as a

shock tube with an area change at the diaphram section. Because of the bulging of the diaphragm prior to rupture it can be further assumed that the entrance to the smaller flow section can be approximated by a convergent nozzle. The required theory for this type of shock tube is well understood and can be found in such publications as that by Alpher and White (1958) which shows that for the same diaphragm pressure ratio, a stronger shock than that in a constant area shock tube is predicted.

EXPERIMENTAL APPARATUS

The shock tube used for the experimental study consists of a 102 mm diameter tube with a total length of 670mm. The length is made up of a 460mm long section and four other interchangeable sections with various lengths to allow the use of the shock tube in different configurations with the ability to place the diaphragms at any chosen section. Several different shock tube diaphragms were used ranging from polyester film (Mylar®) of various thicknesses up to 0.18mm and aluminum 50 microns in thickness, with 12 micron Mylar for the movable wall.

RESULTS

Meyer (1957) demonstrated close agreement between theory and experiment for the case of a well defined constant area shock reflecting off a moving wall. The purpose of the present experimental study is to test the validity of the simplified model described above to cover the case where the moving wall is in close proximity to an incompletely open shock tube diaphragm.

In preliminary experiments to determine the pressure acting on the upstream surface of the movable wall, a PCB piezo-electric pressure transducer was employed to measure the pressure downstream of the bursting diaphragm at the centre of the tube. The pressure measured was that behind the shock wave reflecting off the surface of the transducer which is a flat surface 5.6mm in diameter. When the transducer was only 10mm downstream of the diaphragm position it recorded a pressure approximately double the pressure registered when it was 500mm downstream of the diaphragm. It is clear from the results that at very close proximity to the bursting diaphragm the pressure available to accelerate the wall is much stronger.

For a more detailed study of the flow from an incompletely opened shock tube diaphragm, thermocouple probes are being developed which will allow spatial resolution of the local shock strength in the near vicinity of the bursting diaphragm. The probes consist of a pair of thermocouples spatially separated in a direction parallel to the shock tube axis so as to allow differential shock timing.

Preliminary results have been obtained with 50 micron welded junction rhodium - platinum thermocouples mounted in 0.4mm O.D stainless steel hollow tubing. These proved robust and simple to mount in the shock tube. Sample results are shown in figure 6. Details of the two traces clearly show the arrival of the incident shock and also the reflected shock from the plate supporting the probe. This design therefore shows great promise for the exploration of the shock pattern issuing from a shock tube diaphragm during opening. Further experiments are underway with higher output copper - constantan thermocouples to further improve temporal resolution.

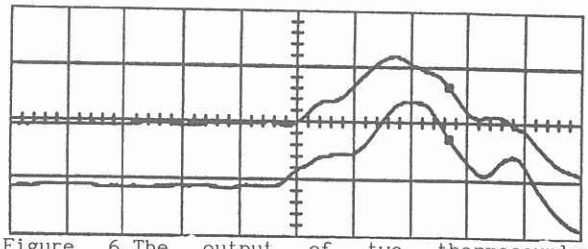

Figure 6. The output of two thermocouples spatially seperated in the direction parallel to the tube axis employed to measure the shock velocity. The Y axis is the voltage output and the X the time.

CONCLUDING REMARKS

The response of a movable wall subject to the incidence of a normal shock wave has been considered. The theory of Meyer has been extended to cover the case of different gases on either side of the wall. This theory indicates that there is little effect on wall acceleration by using a light gas such as helium downstream of the wall rather than, say, air, but there is much higher wall acceleration for higher initial (equal) pressures on either side of the wall.

When the movable wall is located very near the shock tube diaphragm, there is considerable interaction between the diaphragm opening flows and those developing behind the moving wall. This has the effect of causing the shock reflected from the upstream surface of the moving wall to be further reflected at the contact discontinuity. Furthermore, considerable wall movement occurs before the diaphragm is fully opened. This establishes a need to study the shock developing from a partially opened diaphragm. For this purpose, a probe design has been developed and tested which allows for measurements of local shock speed. Further experimentation will be carried out to measure the velocity of the movable wall using laser technology.

ACKNOWLEDGEMENTS

This work has been supported by the ARC.

REFERENCES

1. Alpher, R A. and White, D R (1958) Flow in shock tubes with area change at the diaphragm section. Journal of Fluid Mechanics, 3, 457.

2. Bull, D C and Edwards, D H (1968) An investigation of the reflected shock interaction process in a shock tube, AIAA, 6, pp. 1548-1555.

4. Courant, R and Friedrichs, K O. (1948) Supersonic flow and shock waves, Interscience, New York.

3. Curzon, F L and Phillips, M G R (1971) Low attenuation tube: Driving Mechanism and Diaphram Characteristics. Canadian Journal of Physics. Vol. 49, 1971.

4. Klein, T M , Arentzen, R, Lewis, P A and Fitzpatrick-McElliot S. (1992) Transformation of Microbes, Plants and Animals by Particle Bombardment, Biotechnology, **10**, 286-291

5. Meyer, R F (1957) the impact of a shock wave on a movable wall. J. Fluid Mechanics, 3, 309.

6. Morgan, R G and Stalker, R J (1991) Double Diaphragm Driven Free Piston Expansion Tube, 18th Int. Shock Tube Symp., Sedia Japan, 1991

7. Simpson, C J S M , Chandler, T R D and Bridgman, K B(1967) Effect on shock trajectory of the opening time of a diaphragm in a shock tube. The Physics of Fluids, vol. 10, number 9 .